Enhanced terahertz magnetic dipole response by subwavelength fiber (F)

Shaghik Atakaramians (iD), Ilya V. Shadrivov (iD), Andrey E. Miroshnichenko, Alessio Stefani (iD), Heike Ebendorff-Heidepriem, Tanya M. Monro, and Shahraam Afshar V.

COLLECTIONS

F   This paper was selected as Featured

View Online   Export Citation   CrossMark

ARTICLES YOU MAY BE INTERESTED IN

Tutorial: Terahertz beamforming, from concepts to realizations
APL Photonics 3, 051101 (2018); https://doi.org/10.1063/1.5011063

Invited Article: Channel performance for indoor and outdoor terahertz wireless links
APL Photonics 3, 051601 (2018); https://doi.org/10.1063/1.5014037

Invited Article: Narrowband terahertz bandpass filters employing stacked bilayer metasurface antireflection structures
APL Photonics 3, 051602 (2018); https://doi.org/10.1063/1.5003984

Enhanced terahertz magnetic dipole response by subwavelength fiber

Shaghik Atakaramians,[1,2,a] Ilya V. Shadrivov,[3] Andrey E. Miroshnichenko,[4] Alessio Stefani,[2,5] Heike Ebendorff-Heidepriem,[6] Tanya M. Monro,[6,7] and Shahraam Afshar V.[6,7]

[1]*School of Electrical Engineering and Telecommunications, The University of New South Wales Sydney, Sydney, NSW 2052, Australia*
[2]*Institute of Photonics and Optical Science, School of Physics, The University of Sydney, Sydney, NSW 2006, Australia*
[3]*Nonlinear Physics Centre, Australian National University, Canberra, ACT 2601, Australia*
[4]*School of Engineering and Information Technology, University of New South Wales, Canberra, ACT 2600, Australia*
[5]*DTU Fotonik, Department of Photonics Engineering, Technical University of Denmark, DK-2800 Kongens Lyngby, Denmark*
[6]*ARC Centre of Excellence for Nanoscale BioPhotonics (CNBP), Institute for Photonics and Advanced Sensing (IPAS), School of Physical Sciences, The University of Adelaide, Adelaide, South Australia 5005, Australia*
[7]*Laser Physics and Photonic Devices Laboratories, School of Engineering, University of South Australia, Mawson Lakes, SA 5095, Australia*

Dielectric sub-wavelength particles have opened up a new platform for realization of magnetic light. Recently, we have demonstrated that a dipole emitter by a sub-wavelength fiber leads to an enhanced magnetic response. Here, we experimentally demonstrate an enhanced magnetic dipole source in the terahertz frequency range. By placing the fiber next to the hole in a metal screen, we find that the radiation power can be enhanced more than one order of magnitude. The enhancement is due to the excitation of the Mie-type resonances in the fiber. We demonstrate that such a system is equivalent to a double-fiber system excited by a magnetic source. This coupled magnetic dipole and optical fiber system can be considered a unit cell of metasurfaces for manipulation of terahertz radiation and is a proof-of-concept of a possibility to achieve enhanced radiation of a dipole source in proximity of a sub-wavelength fiber. It can also be scaled down to optical frequencies opening up promising avenues for developing integrated nanophotonic devices such as nanoantennas or lasers on fibers. © *2018 Author(s). All article content, except where otherwise noted, is licensed under a Creative Commons Attribution (CC BY) license (http://creativecommons.org/licenses/by/4.0/).* https://doi.org/10.1063/1.5010348

I. INTRODUCTION

Subwavelength dielectric structures provide a platform for strong light matter interaction with breakthrough application in nanoantennas, nanolasers, metasurfaces, and metadevices.[1] At optical frequencies, it has been shown that dielectric nanoparticles lead to strong light localization when excited by a plane wave due to excitation of Mie resonances.[1] These resonances show strong electric and/or magnetic responses that can be leveraged in designing metadevices. As a new twist, we have recently shown that a dipole emitter can also excite the resonances of a nanofiber and lead to strong electric and/or magnetic responses.[2] These responses were represented by the enhanced resonant emission dominated by magnetic dipole excitation. This novel 2D fiber-based platform,

---

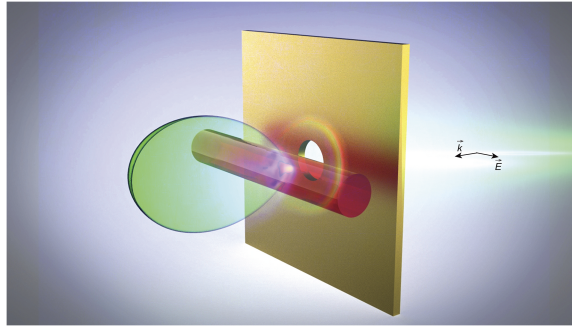[a]Electronic mail: s.atakaramians@unsw.edu.au

FIG. 1.   Schematic of the problem. Aperture in a metallic screen with a dielectric fiber placed on top act as a magnetic dipole emitter when excited by a wave incident on the aperture.

invariant along the fiber and confined with subwavelength scales in the other dimension, not only has enhanced electric and magnetic responses similar to subwavelength particles due to the excitation of Mie resonances but also allows harnessing the guided waves of fibers opening up a new horizon for designing integrated metadevices.

Modification of the radiation characteristics of a source by the electromagnetic environment is one of the most important discoveries of the twentieth century. In particular, change of the emitter's lifetime by a resonator is associated with the *Purcell effect*,[3] which was originally demonstrated for magnetic dipole (MD) type sources in the microwave frequency range. While the modification of an electric dipole (ED) source in the optical domain by the photonic systems has been studied extensively, the modification of an MD source has gained momentum only recently with the aim of developing ultra-efficient optical devices using the magnetic nature of light.[1,4] There have been rigorous theoretical studies[5–10] and experimental confirmation[11–15] of ED emission demonstrating that the strong Purcell effect can be achieved when the emitter is placed within microcavities,[11,16] in photonic crystals,[11,12] in hot spots of nanoantennas,[17–19] fibers,[10] and metamaterials.[7,13,15] Recently there has been great interest in investigating the MD emission enhancement,[20] with the aim of exploiting the Purcell effect in the visible spectrum. Several effects were observed, including strong MD transitions,[21–23] possibility of selective excitation of these transitions[24,25] and strong magnetic response of nanoparticles.[1] Similarly, the Purcell enhancement of MD emitters located in or near various photonic systems[20] including bulk materials, planar structures,[20] maser cavity,[26] nanoplasmonic[27,28] and all dielectric[29,30] nanoantennas, and metamaterials[31–33] has been studied in either microwave or optics. To the best of our knowledge, there is no report on the Purcell factor enhancement of MD emitters in the vicinity of fibers, while the enhancement of ED emitters in the vicinity of fibers has been studied.[2,9,10] Furthermore, there is no report on the MD Purcell effect in the THz range as the realization of MD antennas at higher frequencies (including THz range and optics) are difficult, both because of the reduced sizes of the antennas as well as difficulty associated with feeding such antennas.

In this paper, we experimentally demonstrate the magnetic dipole radiation enhancement for the structure containing a hole in a metallic screen[34] and a dielectric subwavelength fiber, as shown in Fig. 1. This experiment is not only the first proof-of-concept of radiation enhancement of an MD dipole source in the vicinity of a subwavelength fiber but also the first observation of the Purcell effect for a magnetic dipole source in the THz frequency range. This hybrid platform of aperture and fiber can be further expanded into an array configuration opening up a new type of hybrid metasurfaces for manipulating THz and higher frequency radiation. Moreover, utilizing guided modes of the fiber will open up new avenues in developing integrated devices.

II. TERAHERTZ EXPERIMENT AND NUMERICAL SIMULATIONS

A. Subwavelength aperture as a magnetic dipole source

The diffraction of a plane wave by an aperture in a perfectly conducting screen can be represented as a radiation of a series of multipole sources.[35,36] When the dimension of the aperture is small

compared to the wavelength, the aperture acts as the ED and MD source of radiation with the contributions of higher multipoles being negligible.[34,35,37] The effective ED and MD moments can be calculated in terms of integrals of the tangential electric field over the opening of the aperture as follows:[34]

$$\vec{p} = \epsilon\hat{z} \int (\vec{x} \cdot \vec{E}_{\tan})da, \qquad (1)$$

$$\vec{m} = \frac{2}{j\omega\mu} \int (\hat{z} \times \vec{E}_{\tan})da, \qquad (2)$$

where $\vec{E}_{\tan}$ is the tangential electric field in the aperture, $\vec{x}$ is the position vector in the xy-plane, $\hat{z}$ is the unit vector normal to the aperture plane, and the integration is over the area of aperture. It has been shown that the approximation of a subwavelength aperture with effective dipole sources is only valid when the diameter is less than 0.3λ.[38]

Figure 2 shows the normalized ED and MD moments of a 300 μm diameter aperture in the $z = 0$ plane as a function of frequency. We use the commercial software CST Microwave Studio to calculate the tangential component of the electric field in the aperture, when it is excited with an x-polarized plane wave propagating in the z direction. The relative aperture diameter to the wavelength will be 0.3 at $f = 0.3$ THz, beyond which the approximation breaks down [gray shaded region in Fig. 2(b)]. The MD components are normalized to the maximum of y magnetic moment MD_{max}, while the electric component is normalized to MD_{max}/c to be unit less, where c is the speed of light in vacuum. As one clearly observes, the MD_y component is the dominant component ($MD_y/MD_x > 100$ and $MD_y/ED_z > 1000$). This is consistent with what has been reported in the literature,[34,35,37] i.e., for a normal incident plane wave, where the electric and magnetic fields of excitation are parallel to the film, the scattering properties of a sub-wavelength aperture in a metallic film are mainly determined by a magnetic dipole, which is directed appositely to the magnetic field component of the incident plane wave [$\vec{H}$ in Fig. 2(a)].

Although one could argue that the total radiation pattern of the system is angle dependent, i.e., perpendicular to the metallic plane MD_y moment is maximum and ED_z is zero, while at grazing angle MD_y is zero and ED_z is in its maximum, it is safe to consider the system as a MD_y source for this work as, first, MD_y is more than three orders of magnitude stronger and, second, as discussed below,

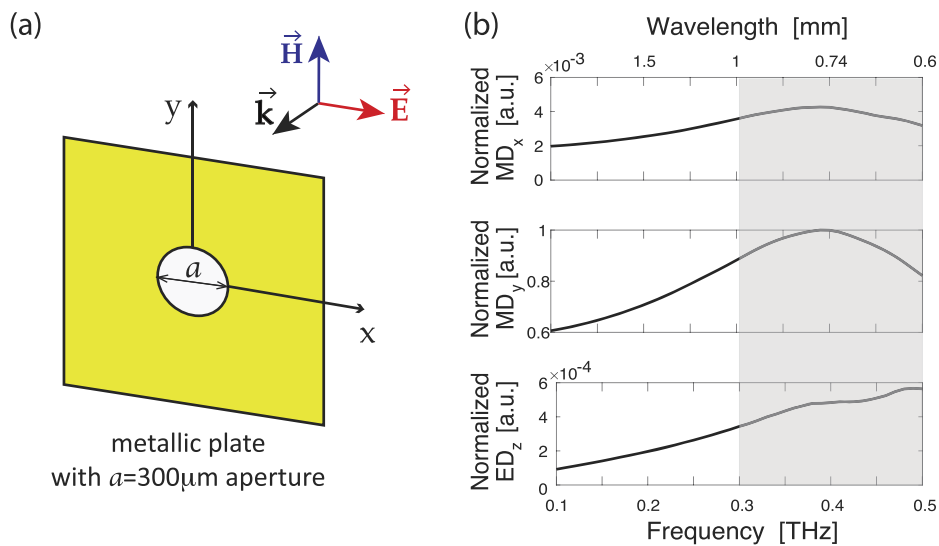FIG. 2. (a) Schematic of a subwavelength aperture in a perfectly conducting plane. (b) The normalized ED and MD moments of a 300 μm diameter aperture at the THz range, when it is excited with an x-polarized plane wave. The gray-shaded area represents the range of frequencies where the approximation of subwavelength aperture with effective dipole sources is not valid.

we are investigating the power flowing through a flat surface parallel to the metallic film, which is mainly along the direction of maximum of MD_y and zero of ED_z radiations.

B. Aperture-fiber system: Experiment and simulation

We use THz time domain spectroscopy (THz-TDS) to conduct our experiment, enhanced MD radiation in the vicinity of sub-wavelength fibers. The TDS system comprises two photoconductive antennas (a common H-shaped antenna with a Si lens on top for generation and a near-field microprobe tip[39] for detection) pumped by a mode-locked Ti:sapphire laser. The near-field microprobe introduces a minimum distortion to the field structure as was shown in previous studies.[40–42] The generated THz electric field is linearly polarized [in this case, x-polarized as shown in Fig. 3(a)] and it is focused on the center of a 300 μm aperture in a very thin (<100 μm) copper plate using two plastic lenses. The detector is moved in the xy-plane to generate a near-field raster image of the transmitted electric field. The scan is conducted over a square area of 850×850 μm^2 with 0.03 mm step size in both directions. The same step size was used for time delay leading into 14 GHz frequency resolution. A 300 μm diameter soft glass microfiber, known as F2, is used for this experiment. The chosen soft glass has a relatively medium refractive index ($n = 2.7$) and material loss <10 cm^{-1} at the interested frequency range.[43] It is worth highlighting that the numerical modeling has shown that the maximum enhancement in the transmission is achieved when the diameter of the fiber is chosen to be identical to
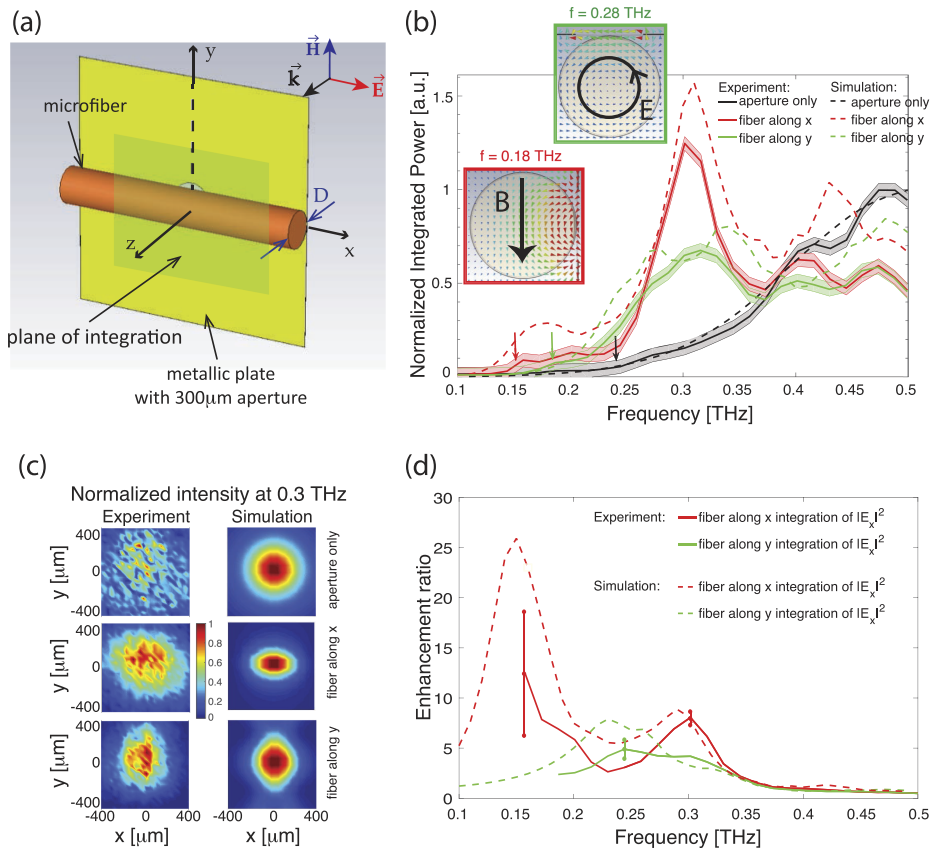

FIG. 3. (a) Schematic of the aperture-fiber system. (b) Normalized integrated power over the raster scan area: experiment (solid lines) and numerical simulation (dashed lines). The shaded area represents the error due to the noise. The insets show the vector magnetic and electric field distributions at the position of the first numerical peak for each curve. (c) Normalized electric field intensity at 0.3 THz measured experimentally (first column) and calculated numerically (second column). (d) Enhancement ratio: experiment (solid lines) and numerical simulations (dashed lines). The vertical bars represent the error due to the noise at the position of the peaks.

that of the aperture. We attribute this to the effective coupling of the aperture emission into resonance modes of the system.

The experiment is conducted in three steps. First, the aperture is positioned at the focal point of the beam and the center of the raster scan is determined, where the maximum signal is recorded at the detector. Second, the fiber is positioned on the aperture and the raster scan is taken at 10 μm distance from the fiber (310 μm from the brass plate). Third, the fiber is removed and a reference raster scan is taken from the aperture only at 310 μm distance from the brass plate. All three steps are repeated for two orientation of the fiber [Fig. 3(a)], i.e., fiber parallel to the excitation (fiber along x) and fiber perpendicular to the excitation (fiber along y).

Figure 3(b) shows the measured normalized power integrated over the square area of the raster scan (850 × 850 μm^2) for aperture only (black solid line), and when the fiber is oriented along the x-axis (red solid line) and along the y-axis (green solid line). The curves are normalized to the maximum integrated power through the aperture. Figure 3(b) also shows the simulated normalized power integrated on the same area (dotted lines), where similarly the curves are normalized to the maximum integrated power through the aperture. As expected for a bare aperture, the power gradually increases and reaches its maximum when the diameter is equal to half of the operating wavelength ($a = \lambda/2$), i.e., $f = c/(2a) = 0.5$ THz. With the fiber, the transmitted signal is enhanced for frequencies below 0.36 THz for both orientations. As discussed in our previous studies,[2,10] the enhancement in transmission is due to excitation of Mie resonances in the fiber cross section, which is also the position of the first transverse electric (TE) and magnetic (TM) whispering gallery modes (WGMs) formed at the cross section of the fiber.

The vertical arrows in Fig. 3(b) indicate the points where the signal level falls within the noise level of the system for each measurement and thus experimental results beyond the arrows cannot be trusted. The shift towards lower frequencies of the arrows is consistent with the enhancement of the transmission through the fibers. The experimental and simulation results do not match well above 0.4 THz, the region which is off interest to this work. We attribute this discrepancy between the simulation and experiment to the fact that at higher frequencies the beam width (FWHM = 500 μm at 0.4 THz) becomes comparable to the aperture size and therefore the field uniformity assumption in the aperture is not valid anymore.

Figure 3(c) shows the measured (first column) and numerically calculated (second column) normalized electric field intensity at 0.3 THz for aperture only (first row), microfiber along x (second row), and microfiber along y (third row). The enhancement of the transmitted signal through the aperture-microfiber system can also be visually observed in Fig. 3(c). Moreover, there is a focusing effect perpendicular to the direction of the microfiber due to the focusing effect in the near field.[44] See the supplementary material for the time evolution of THz radiation. Figure 3(d) shows the normalized integrated power for both orientations of microfibers, where curves are normalized to aperture only [black curves in Fig. 3(b)]. We have extrapolated the normalized power of the bare aperture (using the simulation results) for the frequencies in the noise level of the system so that we can calculate the enhancement ratio up to the aperture-fiber system noise level for each case. A relatively good agreement between measured (solid lines) and numerical (dashed lines) results is observed. Two peaks at 0.15 and 0.32 THz correspond to the microfiber along x. At the position of the first peak (at 0.15 THz), more than 12 times enhancement is achieved experimentally, while the numerical simulation predicts more than 20 times enhancement. The enhancement (7 times) and position (at 0.32 THz) of the second peak are in good agreement with the numerical results. When the fiber is along y, there exists a peak at 0.244 THz where the signal is enhanced 5 times, while the numerical simulation predicts 7 times enhancement at 0.23 THz. Note that the near-field probe measures the x-component of the electric field; therefore all the simulation results presented so far are also considering the x-component of the electric field only.

There are a few factors that can contribute to the discrepancy between the measured (solid curves) and simulated (dashed curves) results: the relative alignment of the microfiber and aperture, the extrapolation of aperture only curve ($f < 0.25$ THz), and the signal being close to the noise level of the system. The simulation results confirm that a 30–50 μm misalignment of the microfiber with respect to the aperture can lead into 6%–10% drop in the enhancement ratio. The slight horizontal shift of the peaks is less than the frequency resolution of the scan. Although increasing the time delay

might give better resolution, it will add the uncertainty of power changes of the laser source into the measurements. As stated earlier, observed enhancement is due to excitation of Mie resonances. However, the positions of the peaks in the enhanced ratio (also in the scattering cross section of the system) are shifted compared to the positions of the first resonances of the Mie scattering coefficient of a single isolated cylinder.[45] As we explained in Sec. II C, this is due to the existence of the mirror image of the fiber, which results into near-field coupling of electric field of the system resonances and leads to the shift of the resonance.

C. MD-double fiber: Equivalent system and discussion

We have demonstrated that a subwavelength fiber excited by an ED can be modeled in the vicinity of the first radiation peak by an effective ED or MD depending on the relative orientation of the dipole source and the fiber.[2] This happens due to excitation of the electric and magnetic Mie resonances overlapping with the position of the first TE and TM WGMs formed at the cross section of the fiber.[10] It is expected that an MD source also excites Mie resonances (TE and TM WGMs) of the fiber leading into effective induced ED and/or MD modes (depending on the orientation of the source relative to the fiber) similar to what has been observed for transverse oriented ED and MD sources in the vicinity of the nanospheres.[29] In general, the coupling efficiency of an electric and magnetic dipole with TE and TM WGMs is described through $\vec{p} \cdot \vec{E}$ and $\vec{m} \cdot \vec{H}$, respectively ($\vec{p}$ and $\vec{m}$ are electric and magnetic moments, respectively, and $\vec{E}$ and $\vec{H}$ are the electric and magnetic fields of the mode).[10] Hence depending on the direction of dipole, different coupling and enhancement are observed for different source and fiber orientations. In this section, we investigate and compare the numerical results of an equivalent system, consisting of a magnetic dipole as an excitation source, for the aperture-fiber system. Replacing the aperture by a magnetic dipole and using image theory to eliminate the perfect conducting plane lead into a double-fiber equivalent system shown in Fig. 4(a).

Based on the image theory, the reflection of ED and MD parallel to a perfect conductor is antiparallel and parallel to the source, respectively. To take care of image sources after removing the perfectly conducting plane, we introduce a second fiber, corresponding to a mirror image of the fiber with respect to the conductor plane. For an MD source located in the middle and parallel to the fibers
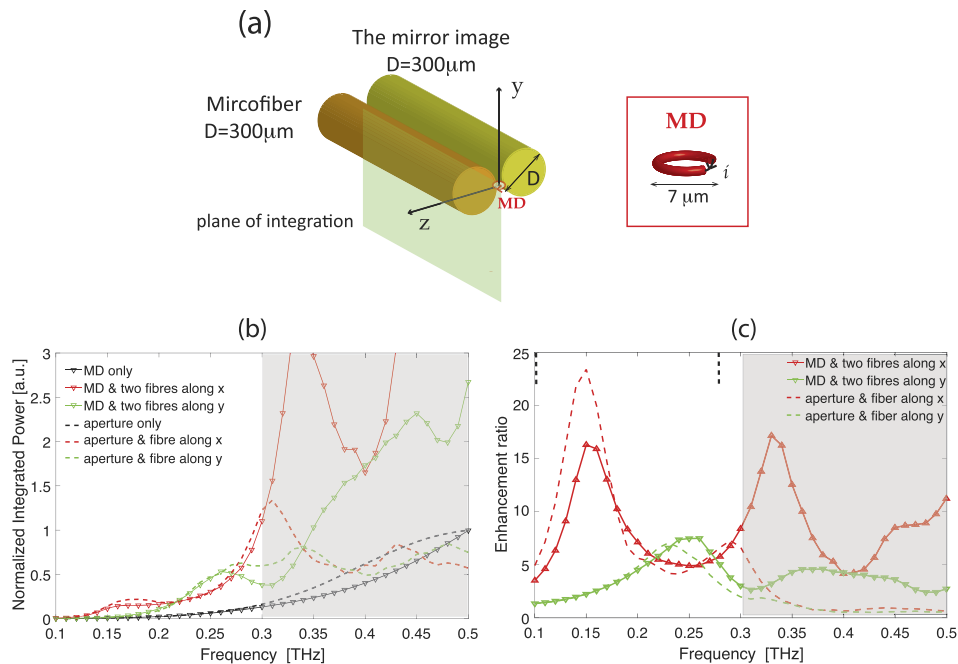

FIG. 4. (a) Schematic of an equivalent system for aperture-fiber systems. (b) Normalized integrated power over the raster scan area: equivalent system (solid lines with markers) and aperture-fiber system (dashed lines). (c) Enhancement ratio; vertical dashed lines show the position of the first two Mie resonances. The gray-shaded area represents the range of frequencies where the approximation of subwavelength aperture with effective dipole sources is not valid.

axis (along z), the induced MD inside the fibers will be along the same directions, while for an MD source transverse to the fibers (along y), the induced ED in the both fibers will be antiparallel.

We have designed the THz MD source using a subwavelength loop (7 μm diameter) excited by a current source, Fig. 4(a). The fibers are positioned 9 μm apart resulting into a 1 μm gap between MD and each fiber (negligible compared to the wavelength). The normalized integrated power on a similar square area as the raster scan (850 × 850 μm^2 and 10 μm away from the fiber) for the MD source only and MD-double fiber system (when fibers are along the x and y axes) are shown in Fig. 4(b). The curves for all three cases are normalized to the integrated power of the MD source at 0.5 THz. The results exhibit a similar trend to that of the simulation results for the aperture-fiber system up to 0.3 THz ($a/\lambda = 0.3$). As discussed above, beyond 0.3 THz [gray-shaded region in Figs. 4(b) and 4(c)], the approximation of the aperture acting as an MD source does not hold anymore.[38] This is apparent from the comparison of black dashed and marked solid lines. The enhancement ratio for both orientations is shown in Fig. 4(c), where the results are in good agreement for the first peaks. This indicates that the system is equivalent to an MD and double-fiber system. The vertical dashed black lines show the position of Mie resonance of an infinitely long fiber,[2,45] which as mentioned do not overlap with the enhancement points of the system. The peaks observed in the system are shifted due to existence of the mirror image of the fiber leading into coupling of the Mie resonances of the two fibers in the near field. Note that we have observed an 8%-10% decrease in the first peak magnitudes when the power is integrated over a large sphere or infinite plane instead of the square plane of integration. This indicates that the enhancement ratio in Fig. 3(d) can be a reasonable first order approximation of the MD Purcell enhancement of the aperture-fiber or equivalently dipole-double fiber system.

III. CONCLUSION

We have experimentally demonstrated that a subwavelength fiber in front of a sub-wavelength aperture unidirectionally enhances the forward emission more than one order of magnitude. We attribute this enhanced emission to the excitation of Mie-type/WGM resonances formed in the cross section of the microfiber. We have demonstrated that the aperture-fiber system is equivalent of an MD-double fiber system. This confirms that the experimentally measured enhancement ratio is a reasonable approximation of the THz Purcell enhancement of an MD source in the vicinity of subwavelength fibers. Presented results confirm that the approximation of field uniformity in the aperture and representation of the aperture as an MD source is a valid description of the system.

The enhancement of forward emission depends on two factors: loss of the fiber material and refractive index. Lower material loss and higher refractive index will enhance the emission further. An ideal material for THz would be silicon (Si) with lower losses and high refractive index compared to the soft glass in this work. However, the required diameter to observe enhancement due to the first Mie resonances in Si fibers is less than 100 μm for THz, which is extremely difficult to achieve with fiber drawing. It is worth noting that if the fiber is replaced by a sphere of the same diameter, similar enhancement of emission is expected due to excitation of Mie resonances of the sphere.[46] The advantage of the fiber system is that it enables the selection of the resonances.

Such a hybrid aperture-fiber system can be used as a unit cell of metasurfaces for tailoring electromagnetic radiation specifically in the THz part of the spectrum which is less developed compared to other frequency ranges. Moreover, this THz experiment is a proof-of-concept of a possibility to achieve enhanced radiation of an MD source coupled to a nanofiber in optics, which has a potential in developing integrated nanophotonic devices such as integrated nanoantennas on fibers and lasers when the fiber is doped with an active material.

SUPPLEMENTARY MATERIAL

See supplementary material for the time evolution of THz radiation passing through aperture only, aperture and fiber along x, and aperture and fiber along y.

ACKNOWLEDGMENTS

[1] Y. Kivshar and A. Miroshnichenko, "Meta-optics with Mie resonances," Opt. Photonics News **28**, 24–31 (2017).

[2] S. Atakaramians, A. E. Miroshnichenko, I. V. Shadrivov, A. Mirzaei, T. M. Monro, Y. S. Kivshar, and S. Afshar V., "Strong magnetic response of optical nanofibers," ACS Photonics **3**, 972–978 (2016).

[3] E. M. Purcell, "Spontaneous emission probabilities at radio frequencies," Phys. Rev. **69**, 681 (1946).

[4] A. I. Kuznetsov, A. E. Miroshnichenko, Y. H. Fu, J. Zhang, and B. Luk'yanchuk, "Magnetic light," Sci. Rep. **2**, 492 (2012).

[5] L. Novotny and B. Hecht, *Principles of Nano-Optics* (Cambridge University Press, 2004).

[6] P. T. Kristensen and S. Hughes, "Modes and mode volumes of leaky optical cavities and plasmonic nanoresonators," ACS Photonics **1**(1), 2–10 (2014).

[7] P. Ginzburg, "Cavity quantum electrodynamics in application to plasmonics and metamaterials," Rev. Phys. **1**, 120–139 (2016).

[8] A. E. Krasnok, A. P. Slobozhanyuk, C. R. Simovski, S. A. Tretyakov, A. N. Poddubny, A. E. Miroshnichenko, Y. S. Kivshar, and P. A. Belov, "An antenna model for the purcell effect," Sci. Rep. **5**(1), 12956 (2015).

[9] M. R. Henderson, S. Afshar V., A. D. Greentree, and T. M. Monro, "Dipole emitters in fiber: Interface effects, collection efficiency and optimization," Opt. Express **19**(17), 16182–16194 (2011).

[10] S. Afshar V., M. R. Henderson, A. D. Greentree, B. C. Gibson, and T. M. Monro, "Self-formed cavity quantum electrodynamics in coupled dipole cylindrical-waveguide systems," Opt. Express **22**, 11301 (2014).

[11] M. Pelton, "Modified spontaneous emission in nanophotonic structures," Nat. Photonics **9**(7), 427–435 (2015).

[12] P. Lodahl, A. F. Van Driel, I. S. Nikolaev, A. Irman, K. Overgaag, D. Vanmaekelbergh, and W. L. Vos, "Controlling the dynamics of spontaneous emission from quantum dots by photonic crystals," Nature **430**(7000), 654–657 (2004).

[13] M. A. Noginov, H. Li, Y. A. Barnakov, D. Dryden, G. Nataraj, G. Zhu, C. E. Bonner, M. Mayy, Z. Jacob, and E. E. Narimanov, "Controlling spontaneous emission with metamaterials," Opt. Lett. **35**(11), 1863–1865 (2010).

[14] K. J. Russell, T.-L. Liu, S. Cui, and E. L. Hu, "Large spontaneous emission enhancement in plasmonic nanocavities," Nat. Photonics **6**(7), 459–462 (2012).

[15] K. Rustomji, R. Abdeddaim, C. M. de Sterke, B. Kuhlmey, and S. Enoch, "Measurement and simulation of the polarization-dependent Purcell factor in a microwave fishnet metamaterial," Phys. Rev. B **95**, 035156 (2017).

[16] M. Pelton, C. Santori, J. Vučković, B. Zhang, G. S. Solomon, J. Plant, and Y. Yamamoto, "Efficient source of single photons: A single quantum dot in a micropost microcavity," Phys. Rev. Lett. **89**, 233602 (2002).

[17] M. Agio, "Optical antennas as nanoscale resonators," Nanoscale **4**(3), 692–706 (2012).

[18] L. Novotny and N. van Hulst, "Antennas for light," Nat. Photonics **5**(2), 83–90 (2011).

[19] P. Bharadwaj, B. Deutsch, and L. Novotny, "Optical antennas," Adv. Opt. Photonics **1**(3), 438 (2009).

[20] D. G. Baranov, R. S. Savelev, S. V. Li, A. E. Krasnok, and A. Alù, "Modifying magnetic dipole spontaneous emission with nanophotonic structures: Modifying magnetic dipole spontaneous emission with nanophotonic structures," Laser Photonics Rev. **11**(3), 1600268 (2017).

[21] Q. Thommen and P. Mandel, "Left-handed properties of erbium-doped crystals," Opt. Lett. **31**, 1803–1805 (2006).

[22] Y. Liu, D. Tu, H. Zhu, and X. Chen, "Lanthanide-doped luminescent nanoprobes: Controlled synthesis, optical spectroscopy, and bioapplications," Chem. Soc. Rev. **42**(16), 6924 (2013).

[23] J. R. Zurita-Sánchez and L. Novotny, "Multipolar interband absorption in a semiconductor quantum dot. II. Magnetic dipole enhancement," J. Opt. Soc. Am. B **19**(11), 2722–2726 (2002).

[24] X. Fang, M. L. Tseng, D. P. Tsai, and N. I. Zheludev, "Coherent excitation-selective spectroscopy of multipole resonances," Phys. Rev. Appl. **5**(1), 014010 (2016).

[25] M. Kasperczyk, S. Person, D. Ananias, L. D. Carlos, and L. Novotny, "Excitation of magnetic dipole transitions at optical frequencies," Phys. Rev. Lett. **114**(16), 163903 (2015).

[26] J. Breeze, K.-J. Tan, B. Richards, J. Sathian, M. Oxborrow, and N. M. Alford, "Enhanced magnetic purcell effect in room-temperature masers," Nat. Commun. **6**, 6215 (2015).

[27] T. Feng, Y. Zhou, D. Liu, and J. Li, "Controlling magnetic dipole transition with magnetic plasmonic structures," Opt. Lett. **36**, 2369–2371 (2011).

[28] D. N. Chigrin, D. Kumar, D. Cuma, and G. von Plessen, "Emission quenching of magnetic dipole transitions near a metal nanoparticle," ACS Photonics **3**(1), 27–34 (2016).

[29] B. Rolly, B. Bebey, S. Bidault, B. Stout, and N. Bonod, "Promoting magnetic dipolar transition in trivalent lanthanide ions with lossless Mie resonances," Phys. Rev. B **85**, 245432 (2012).

[30] P. Albella, M. A. Poyli, M. K. Schmidt, S. A. Maier, F. Moreno, J. J. Sáenz, and J. Aizpurua, "Low-loss electric and magnetic field-enhanced spectroscopy with subwavelength silicon dimers," J. Phys. Chem. C **117**, 13573–13584 (2013).

[31] A. P. Slobozhanyuk, A. N. Poddubny, A. E. Krasnok, and P. A. Belov, "Magnetic purcell factor in wire metamaterials," Appl. Phys. Lett. **104**(16), 161105 (2014).

[32] R. Hussain, S. S. Kruk, C. E. Bonner, M. A. Noginov, I. Staude, Y. S. Kivshar, N. Noginova, and D. N. Neshev, "Enhancing Euˆ3+ magnetic dipole emission by resonant plasmonic nanostructures," Opt. Lett. **40**(8), 1659 (2015).

[33] B. Choi, M. Iwanaga, Y. Sugimoto, K. Sakoda, and H. T. Miyazaki, "Selective plasmonic enhancement of electric- and magnetic-dipole radiations of Er ions," Nano Lett. **16**(8), 5191–5196 (2016).

[34] J. D. Jackson, *Classical Electrodynamics*, 3rd ed. (John Wiley & Sons, Inc., 1998).

[35] H. A. Bethe, "Theory of diffraction by small holes," Phys. Rev. **66**, 163 (1944).

[36] C. J. Bouwkamp, "Diffraction theory," Rep. Prog. Phys. **17**, 35 (1954).

[37] H. Kihm, S. Koo, Q. Kim, K. Bao, J. Kihm, W. Bak, S. Eah, C. Lienau, H. Kim, P. Nordlander, N. Halas, N. Park, and D.-S. Kim, "Bethe-hole polarization analyser for the magnetic vector of light," Nat. Commun. **2**, 451 (2011).

[38] F. J. García de Abajo, "Light transmission through a single cylindrical hole in a metallic film," Opt. Express **10**(12), 1475–1484 (2002).

[39] S. Atakaramians, S. Afshar V., T. M. Monro, and D. Abbott, "Terahertz dielectric waveguides," Adv. Opt. Photonics **5**, 169 (2013).

[40] M. Wächter, M. Nagel, and H. Kurz, "Tapered photoconductive terahertz field probe tip with subwavelength spatial resolution," Appl. Phys. Lett. **95**, 041112 (2009).

[41] S. Atakaramians, S. Afshar V., H. Rasmussen, O. Bang, T. M. Monro, and D. Abbott, "Direct probing of evanescent field for characterization of porous terahertz fibers," Appl. Phys. Lett. **98**, 121104 (2011).

[42] M. S. Habib, A. Stefani, S. Atakaramians, S. C. Fleming, A. Argyros, and B. T. Kuhlmey, "A prism based magnifying hyperlens with broad-band imaging," Appl. Phys. Lett. **110**, 101106 (2017).

[43] W. Withayachumnankul, G. M. Png, X. Yin, S. Atakaramians, I. Jones, H. Lin, B. S. Y. Ung, J. Balakrishnan, B. W.-H. Ng, B. Ferguson, S. P. Mickan, B. M. Fischer, and D. Abbott, "T-ray sensing and imaging," Proc. IEEE **95**, 1528–1558 (2007).

[44] B. S. Luk'yanchuk, R. Paniagua-Domínguez, I. Minin, O. Minin, and Z. Wang, "Refractive index less than two: Photonic nanojets yesterday, today and tomorrow," Opt. Mater. Express **7**(6), 1820 (2017).

[45] J. A. Schuller, R. Zia, T. Taubner, and M. L. Brongersma, "Metamaterials based on electric and magnetic resonances of silicon carbide particles," Phys. Rev. Lett. **99**, 107401 (2007).

[46] J. M. M. Hall, M. R. Henderson, N. Riesen, T. M. Monro, and S. Afshar V., "Unified theory of whispering gallery multilayer microspheres with single dipole or active layer sources," Opt. Express **25**, 6192 (2017).